Washington University School of Medicine
Digital Commons@Becker

Open Access Publications

2014

CNS Amyloid-β, Soluble APP-α and-β Kinetics during BACE Inhibition

Justyna A. Dobrowolska
Washington University School of Medicine in St. Louis

Bruce W. Patterson
Washington University School of Medicine in St. Louis

Robert Chott
Washington University School of Medicine in St. Louis

Vitality Ovod
Washington University School of Medicine in St. Louis

Yuriy Pyatkivskyy
Washington University School of Medicine in St. Louis

See next page for additional authors

Follow this and additional works at: http://digitalcommons.wustl.edu/open_access_pubs

Recommended Citation

Dobrowolska, Justyna A.; Patterson, Bruce W.; Chott, Robert; Ovod, Vitality; Pyatkivskyy, Yuriy; Wildsmith, Kristin R.; Kasten, Tom; Yarasheski, Kevin E.; Bateman, Randall J.; and et al, ,"CNS Amyloid-β, Soluble APP-α and-β Kinetics during BACE Inhibition." The Journal of Neuroscience.34,24. 8336-8346. (2014).
http://digitalcommons.wustl.edu/open_access_pubs/2988

This Open Access Publication is brought to you for free and open access by Digital Commons@Becker. It has been accepted for inclusion in Open Access Publications by an authorized administrator of Digital Commons@Becker. For more information, please contact engeszer@wustl.edu.

Authors
Justyna A. Dobrowolska, Bruce W. Patterson, Robert Chott, Vitality Ovod, Yuriy Pyatkivskyy, Kristin R. Wildsmith, Tom Kasten, Kevin E. Yarasheski, Randall J. Bateman, and et al

This open access publication is available at Digital Commons@Becker: http://digitalcommons.wustl.edu/open_access_pubs/2988

Cellular/Molecular

CNS Amyloid-β, Soluble APP-α and -β Kinetics during BACE Inhibition

Justyna A. Dobrowolska,[1] Maria S. Michener,[5] Guoxin Wu,[3] Bruce W. Patterson,[2] Robert Chott,[2] Vitaliy Ovod,[1] Yuriy Pyatkivskyy,[1] Kristin R. Wildsmith,[1] Tom Kasten,[1] Parker Mathers,[5] Mandy Dancho,[5] Christina Lennox,[5] Brad E. Smith,[5] David Gilberto,[5] Debra McLoughlin,[8] Daniel J. Holder,[7] Andrew W. Stamford,[6] Kevin E. Yarasheski,[2] Matthew E. Kennedy,[4] Mary J. Savage,[3] and Randall J. Bateman[1]

[1]Departments of Neurology and [2]Medicine, Washington University School of Medicine, St. Louis, Missouri 63110 and [3]Molecular Biomarkers, [4]Neuroscience, [5]Safety and Laboratory Animal Resources, [6]Medicinal Chemistry, [7]Early Development Statistics, and [8]Preclinical Drug Metabolism, Merck Research Laboratories, West Point, Pennsylvania 19486 and Kenilworth, New Jersey 07033

BACE, a β-secretase, is an attractive potential disease-modifying therapeutic strategy for Alzheimer's disease (AD) as it results directly in the decrease of amyloid precursor protein (APP) processing through the β-secretase pathway and a lowering of CNS amyloid-β (Aβ) levels. The interaction of the β-secretase and α-secretase pathway-mediated processing of APP in the rhesus monkey (nonhuman primate; NHP) CNS is not understood. We hypothesized that CNS inhibition of BACE would result in decreased newly generated Aβ and soluble APPβ (sAPPβ), with increased newly generated sAPPα.

A stable isotope labeling kinetics experiment in NHPs was performed with a $^{13}C_6$-leucine infusion protocol to evaluate effects of BACE inhibition on CNS APP processing by measuring the kinetics of sAPPα, sAPPβ, and Aβ in CSF. Each NHP received a low, medium, or high dose of MBI-5 (BACE inhibitor) or vehicle in a four-way crossover design. CSF sAPPα, sAPPβ, and Aβ were measured by ELISA and newly incorporated label following immunoprecipitation and liquid chromatography-mass spectrometry. Concentrations, kinetics, and amount of newly generated APP fragments were calculated.

sAPPβ and sAPPα kinetics were similar, but both significantly slower than Aβ. BACE inhibition resulted in decreased labeled sAPPβ and Aβ in CSF, without observable changes in labeled CSF sAPPα. ELISA concentrations of sAPPβ and Aβ both decreased and sAPPα increased. sAPPα increased by ELISA, with no difference by labeled sAPPα kinetics indicating increases in product may be due to APP shunting from the β-secretase to the α-secretase pathway. These results provide a quantitative understanding of pharmacodynamic effects of BACE inhibition on NHP CNS, which can inform about target development.

Key words: **amyloid beta; amyloid precursor protein; BACE inhibitor; sAPPα; sAPPβ; SILK**

Introduction

Amyloid precursor protein (APP) is a ubiquitous transmembrane protein involved in cell signaling, development, and gene regulation. Compared with peripheral, non-CNS tissues, CNS APP processing demonstrates increased β-secretase (BACE) activity (Irizarry et al., 2001; Fukumoto et al., 2002) and different responses to γ-secretase modulation (Cook et al., 2010). The differences between APP processing in the CNS and peripheral compartments are not fully understood (Ortega et al., 2013); further understanding of APP processing may be important to inform the design and development of Alzheimer's disease (AD) therapeutics.

APP is first cleaved by either BACE or α-secretase enzyme generating extracellular soluble APP-β (sAPPβ) or sAPPα, respectively (Fig. 1). Following BACE cleavage, the APP C-terminal fragment C99 can be cleaved by γ-secretase producing extracellular amyloid-β (Aβ) and the remaining APP intracellular C-terminal domain. Recent reports (Cook et al., 2010; Portelius et al., 2011) indicate there is an alternate pathway of a tandem α-secretase and BACE cleavage of APP, which results in APP metabolites such as Aβ1–15/1–16. The relationship of physiological α-secretase to BACE processing in the CNS is not fully un-

Received Jan. 30, 2014; revised April 25, 2014; accepted May 5, 2014.

Author contributions: J.A.D., Y.P., K.R.W., M.E.K., M.J.S., and R.J.B. designed research; J.A.D., M.S.M., G.W., R.C., Y.P., K.R.W., P.M., M.D., C.L., B.E.S., D.G., D.M., A.W.S., K.E.Y., and M.E.K. performed research; M.S.M., M.E.K., M.J.S., and R.J.B. contributed unpublished reagents/analytic tools; J.A.D., G.W., B.W.P., R.C., V.O., T.K., D.M., D.J.H., K.E.Y., M.E.K., M.J.S., and R.J.B. analyzed data; J.A.D., B.W.P., and R.J.B. wrote the paper.

The funding for this project was supported by an academic collaborative grant to Washington University and supported by National Institutes of Health (NIH) Grant R01 NS065667 and Merck project support. We would also like to acknowledge these funding sources: NIH support for the Washington University Biomedical Mass Spectrometry Facility (P41 GM103422, P60 DK020579) and the Washington University Nutrition Obesity Research Center (P30 DK056341). We thank Julie Stone (Merck Research Laboratories, West Point, PA) and Eline M.T. van Maanen (Division of Pharmacology Leiden/Amsterdam Center for Drug Research, Leiden University, The Netherlands) for their expertise in modeling discussions.

Funding, antibodies, and reagents were obtained from Merck Research Laboratories. Washington University has pending patents on some of the techniques described in this report.

Correspondence should be addressed to Dr. Randall J. Bateman, Washington University in St. Louis, Department of Neurology, Campus Box 8111, 660 South Euclid Avenue, St. Louis, MO 63110. E-mail: batemanr@wustl.edu.

J. A. Dobrowolska's present address: The Research Institute at Nationwide Children's Hospital, 700 Children's Drive, Columbus, OH 43205.

K. R. Wildsmith's present address: Genentech, Inc., 1 DNA Way, South San Francisco CA 94080.

Y. Pyatkivskyy's present address: Waters Corporation, 34 Maple St., Milford, MA 01757.

DOI:10.1523/JNEUROSCI.0540-14.2014

Copyright © 2014 the authors 0270-6474/14/348336-11$15.00/0

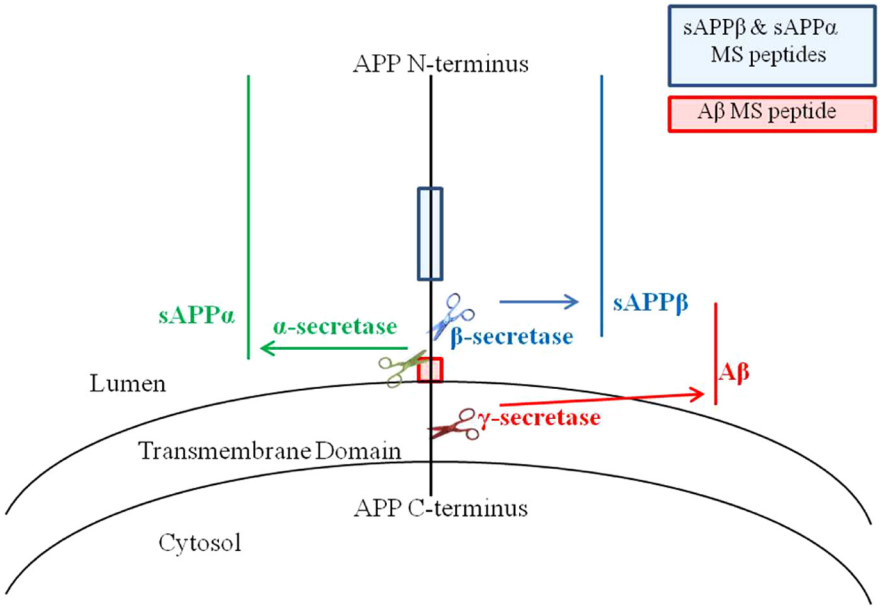

Figure 1. APP and secretase cleavage sites. APP may be cleaved by either β- or α-secretase, and subsequently cleaved by γ-secretase. A concerted β-/γ-secretase cleavage releases Aβ. Indicated on this schematic are the regions of APP where peptides for the SILK study are used to determine labeling of APP metabolites. The sAPPα and sAPPβ peptide (KYLETPGDENEHAHFQ) is in the mid-domain of APP. The Aβ peptide (KLVFFAEDVGSN) is located in the middle of the Aβ sequence. We hypothesize that APP that remains uncleaved by β-secretase due to the presence of a BACE inhibitor will be available for cleavage by α-secretase.

derstood, although some insights from inhibition studies of these enzymes suggest that APP can be shunted to other pathways (Mattsson et al., 2012).

BACE inhibition has been proposed to decrease the amount of APP processed into Aβ, and shunt APP to the α-secretase pathway. BACE1 appears to be the predominant BACE in the CNS and is located mainly in the membranes of cellular compartments. BACE1 may be increased ~2-fold in brains (Fukumoto et al., 2002; Li et al., 2004; Yang et al., 2003) or CSF of AD patients (Holsinger et al., 2006; Verheijen et al., 2006; Zetterberg et al., 2008), although recent reports suggest little change from healthy controls (Wu et al., 2011; Rosén et al., 2012; Savage et al., 2013). Brain penetrant BACE1 inhibitors capable of lowering CNS Aβ in rodent and nonhuman primate (NHP) models (Sankaranarayanan et al., 2009; Malamas et al., 2010; Takahashi et al., 2010; Truong et al., 2010; Cumming et al., 2012; Mandal et al., 2012; Stamford et al., 2012) have been identified and multiple BACE inhibitors have advanced into early stages of human clinical trials (May et al., 2011; Egan et al., 2012, Forman et al., 2013; Bernier et al., 2013).

We sought to determine the kinetic behavior of APP metabolites and the relationship between the α-secretase and BACE pathways during BACE inhibition in rhesus macaques, an NHP model that has 91% homology of APP with human APP. We used stable isotope labeling kinetics (SILK) in combination with a novel high-affinity, selective, and centrally active BACE inhibitor to monitor the production and turnover of APP metabolites. By distinguishing the newly generated metabolites in the CSF from those that previously existed, SILK has provided a more sensitive determination of minute changes in APP metabolites in sporadic and autosomal dominant AD (Mawuenyega et al., 2010; Potter et al., 2013). In the context of γ-secretase inhibition, SILK demonstrated low-dose γ-secretase inhibition effects on Aβ production (Bateman et al., 2009).

Materials and Methods

Cisterna magna ported conscious NHP model. Animal use procedures in this study were reviewed and approved by the Institutional Animal Care and Use Committee at Merck Research Laboratories. They conform to the Guide for the Care and Use of Laboratory Animals (Institute of Laboratory Animal Resources, National Research Council, 1996). The cisterna magna ported (CMP) stable catheterization procedures and CSF flow and collection, as well as the vascular access port infusion protocol, were as described previously (Gilberto et al., 2003; Cook et al., 2010).

$^{13}C_6$-leucine infusion protocol and sample collection. At 48 h before administration of compound or vehicle, monkeys were restricted to a protein-free diet consisting of fruits and vegetables. Protein was reintroduced after the 12 h time point of the study (13 h post dosing of the BACE inhibitor). $^{13}C_6$-leucine infusion procedures were described previously (Cook et al., 2010). Briefly, a 4 mg/kg [U-$^{13}C_6$] leucine priming dose was administered intravenously for 10 min, followed by a steady infusion of 4 mg/kg/h for 12 h. Baseline CSF and blood samples were collected at −22, −20, and −1 h before primed leucine administration. CSF and blood samples were collected at 2, 4, 6, 8, 12, 15, 18, 21, 24, 27, 30, 48, 54, 57, 72, and 144 h after the start of tracer leucine administration. At each time point, a total of 1.5 ml CSF was collected into low-binding polypropylene tubes (Axygen Scientific). The blood was collected into K2 EDTA Vacutainer tubes (Becton Dickinson), spun, and 800 μl of plasma was collected. CSF and plasma samples were then separated into aliquots of lesser volume (into Axygen or standard polypropylene tubes) and placed immediately on dry ice, then stored in a −70°C freezer until analysis.

BACE inhibitor study protocol. The Merck BACE inhibitor, MBI-5 (see Table 1 for pharmacological profile), was used in a four-way crossover randomized design administering one of three doses. Vehicle (0.4% methylcellulose), or 10, 30, and 125 mg/kg MBI-5 was administered orally to conscious CMP NHP ($n = 5$ male rhesus monkeys, 10–13 years old, 8–15 kg) 1 h before initiating the tracer leucine administration. CSF and plasma samples were collected as described above to assess the pharmacokinetics (PK) and pharmacodynamics (PD) of this compound by quantifying MBI-5 concentrations (in plasma and CSF); absolute CSF concentrations of sAPPα, sAPPβ, Aβ_{1-40}, and Aβ_{1-42} (as measured by ELISA); or $^{13}C_6$-leucine/$^{12}C_6$-leucine-labeled CSF sAPPα, sAPPβ, and total Aβ; and free $^{13}C_6$-leucine/$^{12}C_6$-leucine enrichment in plasma. Vehicle/BACE inhibitor administration and sample collection took place at Merck Research Laboratories. Subsequent PK analyses and CSF ELISA measurements also took place at Merck, whereas CSF and plasma were shipped on dry ice to Washington University for SILK analyses: all serial immunoprecipitation (IP)/mass spectrometry (MS) analyses, as well as analyses of total leucine enrichment. Cell culture to generate APP standards for SILK also took place at Washington University.

Cell culture to generate $^{13}C_6$-leucine/$^{12}C_6$-leucine APP fragment standards. Human H4 neuroglioma cells stably transfected with human APP_{751} (H4-APP_{wt}; courtesy of T. E. Golde, University of Florida, Gainesville) were grown in DMEM (Sigma-Aldrich) for two passages. Leucine-free DMEM (Sigma-Aldrich) was supplemented with a mixture of $^{13}C_6$-leucine + $^{12}C_6$-leucine to generate final media solutions with a range of 0%, 1.25%, 2.5%, 5%, 10%, or 20% $^{13}C_6$-leucine. Total leucine concentrations across the mixtures were identical to standard DMEM (105 mg/L). DMEM solutions were supplemented with 1:50 B-27 and 1% each of penicillin-streptomycin and Zeocin. At the third passage, cells were pooled and split evenly at ~80% confluency in T-75 flasks. The

Table 1. *In vitro* pharmacological profile of the BACE inhibitor, MBI-5

	K_i, IC_{50}, nM, or ED_{50} mg/kg, p.o.
Soluble BACE1	10 ± 1
SolubleBACE2	12 ± 2
Cathepsin D	2700 ± 600
Cathepsin E	26,600 ± 11,000
Pepsin	~70,000
Renin	9000
HEK293 $APP^{swe/lon}$ $A\beta_{40}$ IC_{50}	72 ± 5
HEK293 $APP^{swe/lon}$ $A\beta_{42}$ IC_{50}	24 ± 6
HEK293 $APP^{swe/lon}$ sAPPβ IC_{50}	230
Rat plasma $A\beta_{1-40}$	0.4
Rat CSF $A\beta_{1-40}$	8
Rat cortex $A\beta_{1-40}$	23

H4-APP_{wt} cells were reconstituted in one of the six prepared media solutions and cultured for 24 h to allow for sufficient incorporation of label into proteins. Following this incubation with labeled DMEM, the media solutions were collected and apportioned into Axygen tubes in 1 ml aliquots and immediately frozen and stored at −80°C until ready to use.

Aβ, sAPPβ, and sAPPα ELISA protocols. The assays for CSF $A\beta_{1-40}$, $A\beta_{1-42}$, sAPPα, and sAPPβ measurement were described previously (Sankaranarayanan et al., 2009; Wu et al., 2011) with some modification in dilution factor. Briefly, CSF was diluted with 3% BSA/PBS at 1:3 for $A\beta_{1-42}$, 1:10 for $A\beta_{1-40}$, and 1:80 for both sAPPβ and sAPPα and used at 100 μl per ELISA well for each analyte measurement. The concentration was calculated based on each standard curve. The absolute concentrations of total Aβ reported herein are derived by adding the absolute concentrations measured by the two individual Aβ ELISAs: $A\beta_{1-40}$ and $A\beta_{1-42}$.

IP and digestion of sAPPβ. IP of sAPPβ from CSF was performed using a rabbit monoclonal antibody that can specifically recognize the KM-neo-epitope of sAPPβ created following the cleavage of APP by BACE. The generation and specificity characterization of the prepared anti-sAPPβ neo-epitope antibody Mrk-61 was previously described (Wu et al., 2011; Wu et al., 2012). Mrk-61 binds exclusively to sAPPβ, and not to sAPPα, in both Western blot and direct immunoassay experiments that use coated recombinant protein. The purified rabbit monoclonal anti-Mrk-61 antibody was conjugated with CNBr-activated Sepharose 4B beads (GE Healthcare) according to the manufacturer's protocol. The activity of the Sepharose 4B-conjugated Mrk-61 antibody was evaluated for IP efficiency with normal NHP CSF following overnight bead incubation and the sAPPβ level in CSF after IP was measured with a sensitive sAPPβ ELISA (Wu et al., 2011). The characterized Mrk-61-Sepharose 4B beads were then reconstituted into a 50% slurry of 0.02% sodium azide in PBS and stored at 4°C.

From each time point, 500 μl of CSF, in parallel with a set of H4-APP_{wt} media isotopic enrichment standards (0, 1.25, 2.5, 5, 10, and 20% $^{13}C_6$-leucine), was diluted 1:1 with 500 μl PBS. Protease inhibitors (40 μg/ml aprotinin and 20 μg/ml leupeptin; Calbiochem/EMD Millipore) were added to each sample at a volume of 10 μl, followed by the addition of 50 μl of Mrk-61 beads.

Samples were rotated for ~22 h at 4°C, then centrifuged (16,837 × *g*) with 925 μl of resulting supernatants collected into new Axygen tubes and stored at 4°C for ~1.5 h until ready for the sAPPα/Aβ immunoprecipitation protocol. The Mrk-61 bead pellets were washed three times with 25 mM ammonium bicarbonate (AmBic), with centrifugation between washes. The supernatants from the bead washes were aspirated after the final rinse and 100 μl of neat formic acid was immediately added to each sample to elute the sAPPβ from the antibody-bead complex. Samples were left for 10 min at 25°C and centrifuged. The formic acid supernatants were transferred to a new Axygen tube and evaporated in a rotary evaporator at 37°C for 30 min. The dried samples were reconstituted with 25 mM AmBic, and 5 ng sequencing-grade metalloendopeptidase (Lys-N; Seikagaku/Associates of Cape Cod) in 25 mM AmBic was added. Extracts were digested for ~20 h on a shaker at 37°C and transferred into autosampler vials.

IP and digestion of sAPPα and Aβ. Before study onset, a mouse monoclonal antibody W0–2 (EMD Millipore; directed against $A\beta_{1-10}$) and a mouse monoclonal antibody HJ5.1 (Washington University, St. Louis, MO; directed against $A\beta_{13-28}$) were covalently bound to CNBr Sepharose 4B beads according to the manufacturer's instructions, then stored in a 50% slurry of 0.02% PBS azide at 4°C before use. The sAPPα/Aβ IP protocol was optimized for maximum sAPPα/Aβ signal from the liquid chromatography-mass spectrometer (LC-MS) system. The above-mentioned CSF samples and H4-APP_{wt} media APP standard supernatants were taken from 4°C and put on ice. To each sample 45 μl W0–2 antibody slurry and 60 μl HJ5.1 antibody slurry were added. Samples were rotated, rinsed, eluted, evaporated, reconstituted, and digested using the same methods applied to the Mrk-61 bead eluates.

Quantitation of peptides by LC-MS. Mid-domain APP peptides specific to sAPPα and sAPPβ (KYL(L*)ETPGDENEHAHFQ), and a mid-domain Aβ peptide (KL(L*)VFFAEDVGSN; Fig. 1) were analyzed on a Thermo-Finnigan LTQ (Thermo Fisher Scientific) equipped with nanoflow electrospray ionization (nano-ESI; New Objective) source. The peptides were separated by reverse phase HPLC using a 2D-LC nanoflow pump (Eksigent) operating in 1D mode at a flow rate of 200 nl/min. Sample (5 μl) was injected onto a PicoFrit column (New Objective) packed to 12 cm with 5 μm Magic $C18_{aq}$ packing material (Michrom Bioresources). Mobile Phase A contained 0.1% formic acid (FA) in water and Mobile Phase B was 0.1% FA in acetonitrile.

Free leucine quantitation by gas-chromatography-mass spectrometry. Plasma $^{13}C_6$-leucine/$^{12}C_6$-leucine enrichment was determined using gas capillary gas chromatography-mass spectrometry (GC-MS; Agilent 6890N gas chromatograph and Agilent 5973N mass selective detector) in negative chemical ionization mode as described previously (Yarasheski et al., 1992; Bateman et al., 2007; Cook et al., 2010), and $^{13}C_6$-leucine enrichment was quantified as a relative measure, tracer to tracee ratio ($^{13}C_6$-leucine/$^{12}C_6$-leucine; Wolfe et al., 2005).

Calculation of labeled APP metabolite ratio. The percentage of labeled metabolite measured using the SILK method was determined by taking the ratio of *b*- and *y*-product ion intensities from the unlabeled metabolite peptide and the labeled peptide. For Aβ, the peptide quantified was KL(L*)VFFAEDVGSN. For sAPPα and sAPPβ, the peptide was KYL(L*)ETPGDENEHAHFQ. Mole fraction label (MFL) was calculated as $MFL = L/(L + U)$, where L and U are the signal intensities for $^{13}C_6$-leucine (labeled) peptides and $^{12}C_6$-leucine (unlabeled) peptides, respectively.

Calculations of fractional synthesis rate and monoexponential slope fractional clearance rate. The fractional synthesis rate (FSR) and monoexponential slope fractional clearance rate (FCR) were quantified for each metabolite as previously reported (Cook et al., 2010). Briefly, FSR for each CSF APP metabolite was calculated as the slope of the labeled metabolite during 2–8 h, divided by the average plasma $^{13}C_6$-leucine enrichment over that time course. The monoexponential slope FCR was computed using the natural logarithm of each labeled metabolite during the clearance phase of the labeled proteins, notably 18–30 h.

Calculation of newly generated APP metabolites. The concentration of newly generated APP metabolites at each time point was calculated as the product of the absolute concentration of a metabolite (determined by ELISA) and the fraction of the metabolite derived from *de novo* synthesis, i.e., the percentage of metabolite labeled ($^{13}C_6$-leucine-peptide/$^{12}C_6$-leucine-peptide ion intensities, established by LC-MS) after normalization to the plasma $^{13}C_6$-leucine/$^{12}C_6$-leucine enrichment, established by GC-MS (Bateman et al., 2009).

Area under the curve and statistical analyses. For each APP analyte and drug exposure, area under the curve (AUC) was calculated using the trapezoid rule, from −1 to 57 h (AUC_{57}) for APP analytes and from 0 to 59 h (AUC_{59}) for drug. These time durations were chosen due to the majority of the drug effects and labeling occurring over this period. To estimate the effect of each active treatment versus vehicle, a linear mixed effects model with fixed effects for treatments and random effects for monkeys was fit to the log (base 2) of AUC_{57}. Estimates of mean differences from vehicle were back-transformed from the log scale to yield percentage differences. Estimation of the linear relationship between each analyte and drug exposure was performed using a mixed effects model like the one above, except with the treatment effects replaced by a slope and intercept for exposure. Error bars reported in the figures rep-

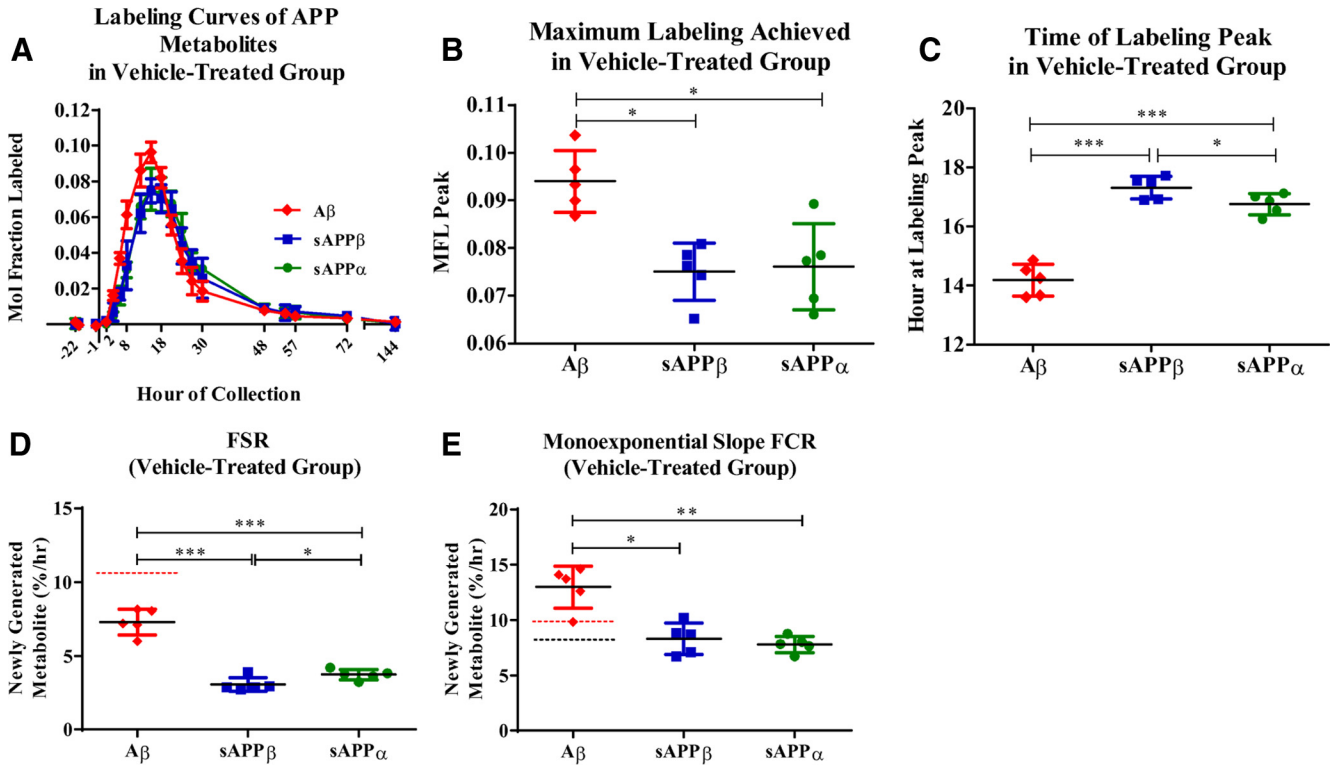

Figure 2. Kinetics of APP metabolites as measured from vehicle-treated NHP CSF ($n = 5$). ***A***, Averaged $^{13}C_6$-leucine labeling curve profiles of sAPPα, sAPPβ, and Aβ. ***B***, Maximum MFL for each metabolite was determined. Aβ reached a significantly higher maximum labeling as compared with sAPPα (paired *t* test, $^*p = 0.02$) and sAPPβ (paired *t* test, $^*p = 0.02$). ***C***, Extrapolated time of maximum labeling was significantly different among metabolites, with Aβ peaking at $t = 14.2$ h, while sAPPα and sAPPβ peaked at $t = 16.76$ h and $t = 17.32$ h, respectively (Aβ vs. sAPPβ: $^{***}p < 0.0005$; Aβ vs. sAPPα: $^{***}p < 0.001$; sAPPβ vs. sAPPα: $^*p = 0.05$). ***D***, Mean FSRs indicating fraction-labeled APP metabolites' appearance in the CSF were significantly different from one another (repeated-measures ANOVA, $^{***}p < 0.0001$). (Aβ vs. sAPPβ: $^{***}p = 0.0002$; Aβ vs. sAPPα: $^{***}p = 0.0006$; sAPPβ vs. sAPPα: $^*p = 0.01$) The red dashed line indicates the previously reported NHP FSR of Aβ (10.7%/h; Cook et al., 2010). ***E***, Mean monoexponential slope FCR of Aβ fraction-labeled loss from CSF was significantly higher than the monoexponential slope FCRs of both sAPPα (paired *t* test, $^{**}p = 0.004$) and sAPPβ (paired *t* test, $^*p = 0.01$). There was no statistically significant difference between sAPPα and sAPPβ monoexponential slope FCRs. The red dashed line indicates previously reported NHP FCR of Aβ (9.9%/h; Cook et al., 2010). The black dashed line indicates previously reported human FCR of Aβ (8.3%/h; Bateman et al., 2006). Error bars indicate SD.

resent SD or SEM (clarified within figure legends). Mean-to-standard deviation (MTSD) values (inverse of coefficient of variation) were calculated using each metabolite's AUC_{57} mean and SD as calculated by SILK, as well as by ELISA. Each metabolite's MTSDs for SILK and ELISA were compared to determine the relative sensitivity of the assays in this study. All analyses and statistical tests were performed in GraphPad Prism version 5.01 for Windows (GraphPad Software) and Microsoft Office Excel 2007. Student's *t* test and repeated-measures analysis of variance (ANOVA) were used to determine whether there were differences among groups in all analyses. Baseline ELISA concentrations of APP metabolites were averaged for each monkey. Means were converted to log values and Pearson correlations between each set of APP metabolites were determined.

Results

Rhesus macaque APP metabolite kinetics

sAPPα and sAPPβ turnover was slower than Aβ in the CSF. The average kinetic curves of sAPPα, sAPPβ, and Aβ in the vehicle-treated group were evaluated (Fig. 2*A*), comparing CSF parameters including maximum MFL and time of maximum peak labeling. Soluble APPα achieved a maximum of 0.076 ± 0.01 (SD) MFL, while sAPPβ exhibited a similar labeling maximum [0.075 ± 0.01 (SD) MFL; $p = 0.76$; Fig. 2*B*]. Aβ had a significantly higher peak of MFL [0.094 ± 0.01 (SD)] compared with both sAPPα and sAPPβ ($^*p = 0.02$ each; Fig. 2*B*). The extrapolated maximum labeling time point for sAPPα and sAPPβ were similar [sAPPα: $t = 16.8 \pm 0.4$ h (SD); sAPPβ: $t = 17.3 \pm 0.4$ h (SD) $^*p = 0.05$], with the Aβ labeling peak significantly earlier [$t = 14.2 \pm 0.5$ h (SD) compared with sAPPβ, $^{***}p < 0.0005$; compared with sAPPα, $^{***}p < 0.001$; Fig. 2*C*].

Kinetic rates of the APP metabolites were estimated using FSR to estimate production rate and monoexponential slope FCR to estimate clearance rate. CSF measures were used throughout as a surrogate for brain rates. FSRs and monoexponential slope FCRs are only valid when measured in a steady-state system (Wolfe et al., 2005), thus kinetic analyses of sAPPα, sAPPβ, and Aβ were performed exclusively using data collected from the vehicle-treated monkeys. The mean sAPPα FSR [3.8 ± 0.4%/h (SD)] was ~18% faster than the mean sAPPβ FSR [3.1 ± 0.5%/h (SD), $^*p = 0.01$; Fig. 2*D*]. The mean Aβ FSR was 7.3 ± 0.9%/h (SD; Fig. 2*D*) and was slightly lower than the previously reported NHP Aβ FSR (dashed red line) of 10.7 ± 0.6%/h (SEM; Cook et al., 2010). The mean Aβ FSR was 58 and 48% faster than that of either sAPPβ ($^{***}p = 0.0002$) or sAPPα ($^{***}p = 0.0006$), respectively.

Mean FCRs for sAPPα and sAPPβ were 7.8 ± 0.7 (SD) and 8.3 ± 1.4%/h (SD), respectively (Fig. 2*E*). Mean Aβ FCR was 13.0 ± 1.9%/h (SD; Fig. 2*E*) and was slightly faster than the previously reported NHP Aβ FCR (dashed red line) of 9.9 ± 0.5% /h (SEM; Cook et al., 2010), as well as approximately twice as fast as mean human Aβ FCR (dashed black line) previously reported (Bateman et al., 2006). The FCRs of all three metabolites were significantly different ($^{**}p < 0.002$) as assessed by a one-way repeated-measures ANOVA. Aβ FCR was significantly faster than FCR of either sAPPβ ($^*p < 0.02$) or sAPPα ($^{**}p < 0.005$), 36 and 40%

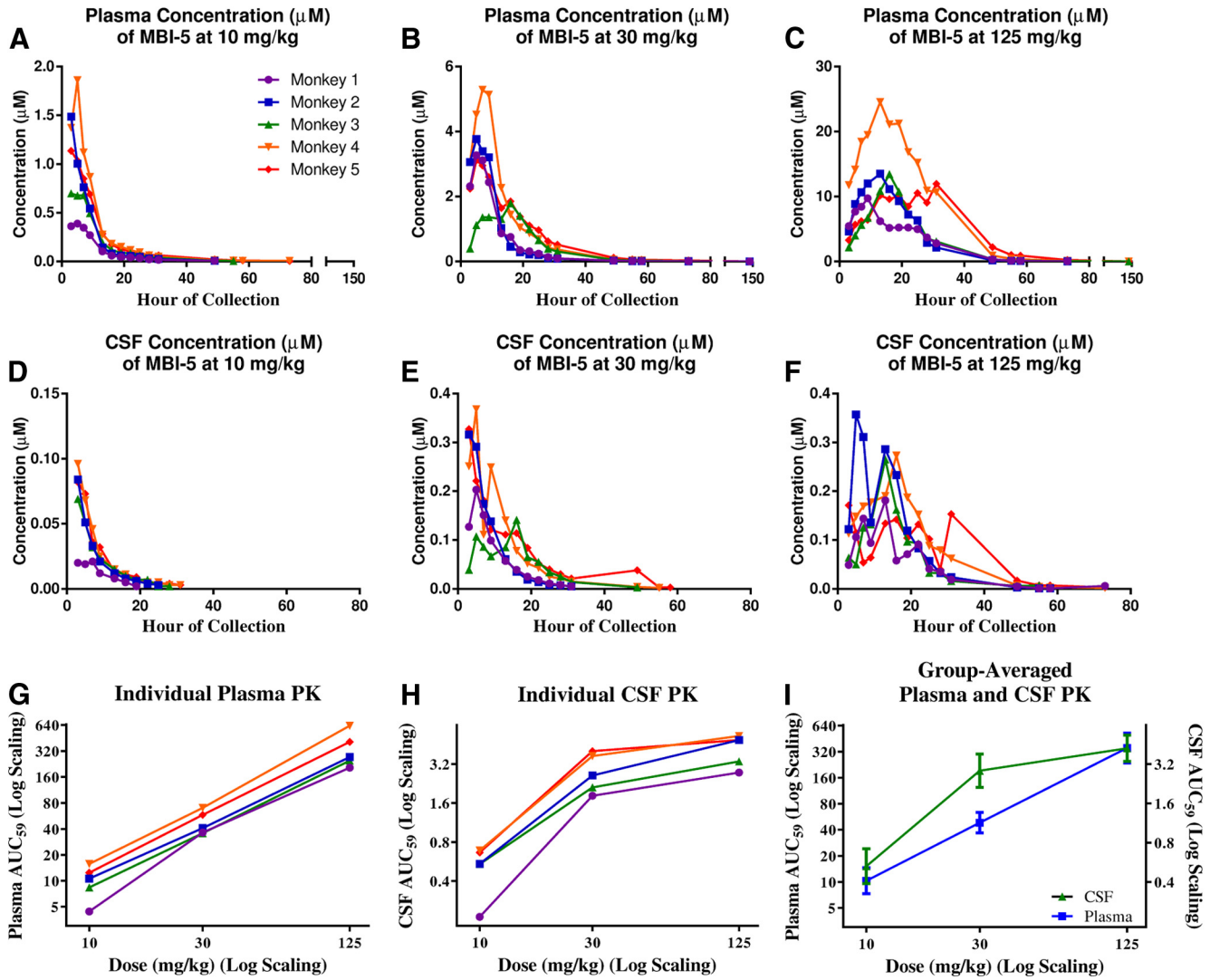

Figure 3. PK of MBI-5 indicate an increase of the BACE inhibitor incorporation into both plasma and CSF with increasing dose. ***A–C***, Individual monkeys' plasma concentrations of MBI-5 after dosing with 10, 30, and 125 mg/kg. ***D–F***, Individual monkeys' CSF concentrations of MBI-5 after dosing with 10, 30, or 125 mg/kg. ***G***, Individual monkeys' plasma AUC_{59} at each dosage. ***H***, Individual monkeys' CSF AUC_{59} at each dosage. ***I***, Group-averaged plasma and CSF PK. Error bars indicate SD.

faster, respectively. The FCRs for sAPPβ and sAPPα were not significantly different from one another ($p = 0.6$). For each metabolite, the FSR is approximately half of the respective FCR. The discrepancy between each metabolite's FSR and FCR is currently being further evaluated by multicompartmental modeling.

Concentrations of MBI-5 were measured in the plasma (Fig. 3*A–C*) and CSF (Fig. 3*D–F*) of each subject to determine the inhibitor's PK at each of the three doses. Individual subjects' AUC_{59} for MBI-5 in plasma (Fig. 3*G*) and in CSF (Fig. 3*H*) were determined. The AUC_{59} was converted to a log scale and plotted against dosage of MBI-5. Group-averaged AUC_{59} for plasma and CSF are plotted against dose in Figure 3*I*. As expected, MBI-5 levels in both plasma and CSF increased with increasing dose, but a linear effect was seen only in plasma. Individual plasma and CSF AUC_{59} C_{max} and T_{max} for each subject at each dose are shown in Tables 2, 3.

Biological variability of APP product concentrations

Some inherent physiological variability of APP metabolites is expected. For each monkey, three baseline concentrations at $t = -22$, -20, and -1 h (before leucine infusion and treatment) of sAPPα, sAPPβ, and Aβ (Aβ_{40} + Aβ_{42}) were measured by ELISA in the vehicle group and each of the experimental groups. The means and SDs are reported in Table 4 and indicate a widespread physiological intra- and inter-monkey variability. sAPPα and sAPPβ concentrations were positively correlated (Pearson $r = 0.98$; $^{**}p = 0.004$; 95% CI: 0.706–0.999). However, Aβ concentrations were not correlated to either sAPPβ (Pearson $r = -0.063$; $p = 0.92$; 95% CI: -0.895 to 0.868) or sAPPα (Pearson $r = -0.098$; $p = 0.88$; 95% CI: -0.902 to 0.859). With small sample size, high precision is not expected, and this is evidenced by the broad 95% CIs for the correlations involving Aβ.

BACE inhibitor dose dependently decreased sAPPβ and Aβ in NHP CSF

Labeling curves of Aβ (Fig. 4*A*) and sAPPβ (Fig. 4*D*), as well as absolute concentrations of both analytes measured by ELISA (Fig. 4*B*,*E*), decreased dose dependently in the presence of a BACE inhibitor. Concentrations of newly generated metabolites were calculated by taking the product of percentage labeled and absolute concentration of a given metabolite at each time point. Similarly to the labeling profiles and absolute concentrations, the

Table 2. Individual monkey plasma PK parameters of MBI-5

Individual plasma PK parameters at 10 mg/kg MBI-5					
Monkey #	1	2	3	4	5
AUC_{59} (nM*h)	4420	106,00	8370	15,700	12,400
C_{max} (nM)	389.3	1487.6	698.8	1860.4	1136.0
T_{max} (h)	5	3	3	5	3
Individual plasma PK parameters at 30 mg/kg MBI-5					
Monkey #	1	2	3	4	5
AUC_{59} (nM*h)	36,300	40,900	35,600	70,100	58,200
C_{max} (nM)	3274.2	3772.4	1792.6	5290.1	3113.8
T_{max} (h)	5	5	16	7	5
Individual plasma PK parameters at 125 mg/kg MBI-5					
Monkey #	1	2	3	4	5
AUC_{59} (nM*h)	205,000	272,000	247,000	628,000	408,000
C_{max} (nM)	9744.8	13512.4	13430.3	24553.9	11961.8
T_{max} (h)	9	13	16	13	31

Table 3. Individual monkey CSF PK parameters of MBI-5

Individual CSF PK parameters at 10 mg/kg MBI-5					
Monkey #	1	2	3	4	5
AUC_{59} (nM*h)	211	541	540	686	663
C_{max} (nM)	20.7	83.8	69.0	95.7	82.4
T_{max} (h)	7	3	3	3	3
Individual CSF PK parameters at 30 mg/kg MBI-5					
Monkey #	1	2	3	4	5
AUC_{59} (nM*h)	1820	2610	2110	3690	4030
C_{max} (nM)	203.2	316.4	140.6	367.7	327.4
T_{max} (h)	5	3	16	5	3
Individual CSF PK parameters at 125 mg/kg MBI-5					
Monkey #	1	2	3	4	5
AUC_{59} (nM*h)	2750	4910	3350	5270	4900
C_{max} (nM)	180.8	356.6	265.3	273.4	171.2
T_{max} (h)	13	5	13	16	3

Table 4. Individual monkeys' baseline sAPPα, sAPPβ, and Aβ concentrations

	pM (SD)		
	Mean baseline sAPPα	Mean baseline sAPPβ	Mean baseline Aβ
Monkey #			
1	1306 (285)	1506 (214)	650 (287)
2	985 (175)	1058 (134)	863 (213)
3	877 (191)	1057 (127)	906 (284)
4	801 (194)	894 (127)	584 (163)
5	1224 (388)	1465 (346)	722 (286)

newly generated Aβ (Fig. 4*C*) and sAPPβ (Fig. 4*F*) reflect a dose-dependent decrease in the presence of a BACE inhibitor. AUC for Aβ or sAPPβ labeling for each monkey after each dose of BACE inhibitor were normalized to each monkey's vehicle labeling curve AUC and averaged. Dose-dependent decreases were observed in AUC_{57} for Aβ and sAPPβ when measured by SILK, by ELISA, and in the newly generated peptide calculations (Table 5).

To determine the relative sensitivity of the assays in this study, we calculated MTSD values for SILK AUC_{57} versus ELISA AUC_{57} for each metabolite. MTSD was always higher for SILK measurements when compared with ELISA, in all doses and for both metabolites. In the cases of highest dose, SILK was clearly more sensitive for sAPPβ ($^*p < 0.05$). The Aβ MTSD was comparable between the two methods used ($p = 0.22$).

Mean values from each BACE inhibitor dosage group for each analyte were compared with the mean value of each vehicle group. The MFL Aβ AUC_{57} ($^{13}C_6$-Aβ/$^{12}C_6$-Aβ) indicated a dose-dependent decrease to ~48% of vehicle at the highest BACE inhibitor dose of 125 mg/kg (Fig. 5*A*, Table 5); ~10% of the total Aβ is labeled. AUCs for ELISA concentrations of Aβ normalized to vehicle showed a dose-dependent response to ~33% of vehicle (Fig. 5*B*, Table 5), a greater extent of reduction than measured by SILK. The newly synthesized Aβ is only ~9% at the highest dosage of BACE inhibitor (Fig. 5*C*, Table 5). SILK MFL sAPPβ AUC_{57} indicated a dose-dependent decrease to a lesser extent than Aβ: ~70% of vehicle values at the highest BACE inhibitor dose (Fig. 5*D*, Table 5), with ~8% of the total sAPPβ being labeled. AUCs for ELISA concentrations of sAPPβ normalized to vehicle showed a dose-dependent response to ~38% of vehicle (Fig. 5*E*, Table 5), a greater extent of reduction than measured by SILK. Similarly to Aβ, AUC_{57} values for newly synthesized sAPPβ indicated a dose-dependent decrease to an even greater extent, ~18% at the highest inhibitor dose, compared with SILK (Fig. 5*F*, Table 5). For graphical representation of AUC_{57} not normalized to the vehicle, please refer to Figure 6.

BACE inhibition had no detectable effect on fraction labeled sAPPα but dose dependently increased total sAPPα concentrations measured by ELISA

The labeling curves of sAPPα for vehicle and all three BACE inhibitor groups indicated no significant differences in sAPPα fraction label (repeated-measures ANOVA, $p = 1.0$; Fig. 4*G*). SILK MFL sAPPα AUC_{57} indicated a lack of significant difference among dosage groups (Fig. 5*G*, Table 5). Concentrations measured by sAPPα ELISA indicated a dose-dependent increase with BACE inhibition (Fig. 4*H*). AUC_{57} for absolute concentrations of sAPPα normalized to vehicle indicated a dose-dependent increase to ~131% at the highest dose (Fig. 5*H*, Table 5). Finally, the newly generated sAPPα (the product of steady-state concentration multiplied by the fraction-labeled sAPPα), demonstrated dose-dependent increases (35%), but to a lesser degree than the observed sAPPβ decrease (83%; Figs. 4*I*, 5*I*, Table 5). Again, to determine the relative sensitivity of the assays in this study, we calculated MTSD values for SILK AUC_{57} versus ELISA AUC_{57} for sAPPα. MTSD was always higher for SILK measurements when compared with ELISA in all doses ($p = 0.053$). For graphical representation of AUC_{57} not normalized to the vehicle, please refer to Figure 6.

Discussion

To date, kinetic behavior of other APP fragments has not been assessed in NHP, although Dobrowolska et al. (2008) demonstrated total sAPP was metabolized ~2-fold slower than Aβ in young, healthy humans. To our knowledge, although some basic APP metabolism has been studied in pulse-chase experiments in various cells lines (Weidemann et al., 1989; Oltersdorf et al., 1990; Busciglio et al., 1993; Perez et al., 1996), there are no prior studies investigating specific sAPPα and sAPPβ metabolism *in vivo*. Here, we present common features of sAPPα and sAPPβ metabolism measured in NHP CSF. Metabolism of these sAPP species, relative to NHP Aβ metabolism, was comparable to findings in humans (Bateman et al., 2006; Dobrowolska et al., 2008) where metabolic rates of both APP species were twice as slow as for Aβ. This correspondence between sAPP metabolism in both species supports rhesus macaques as an appropriate preclinical model

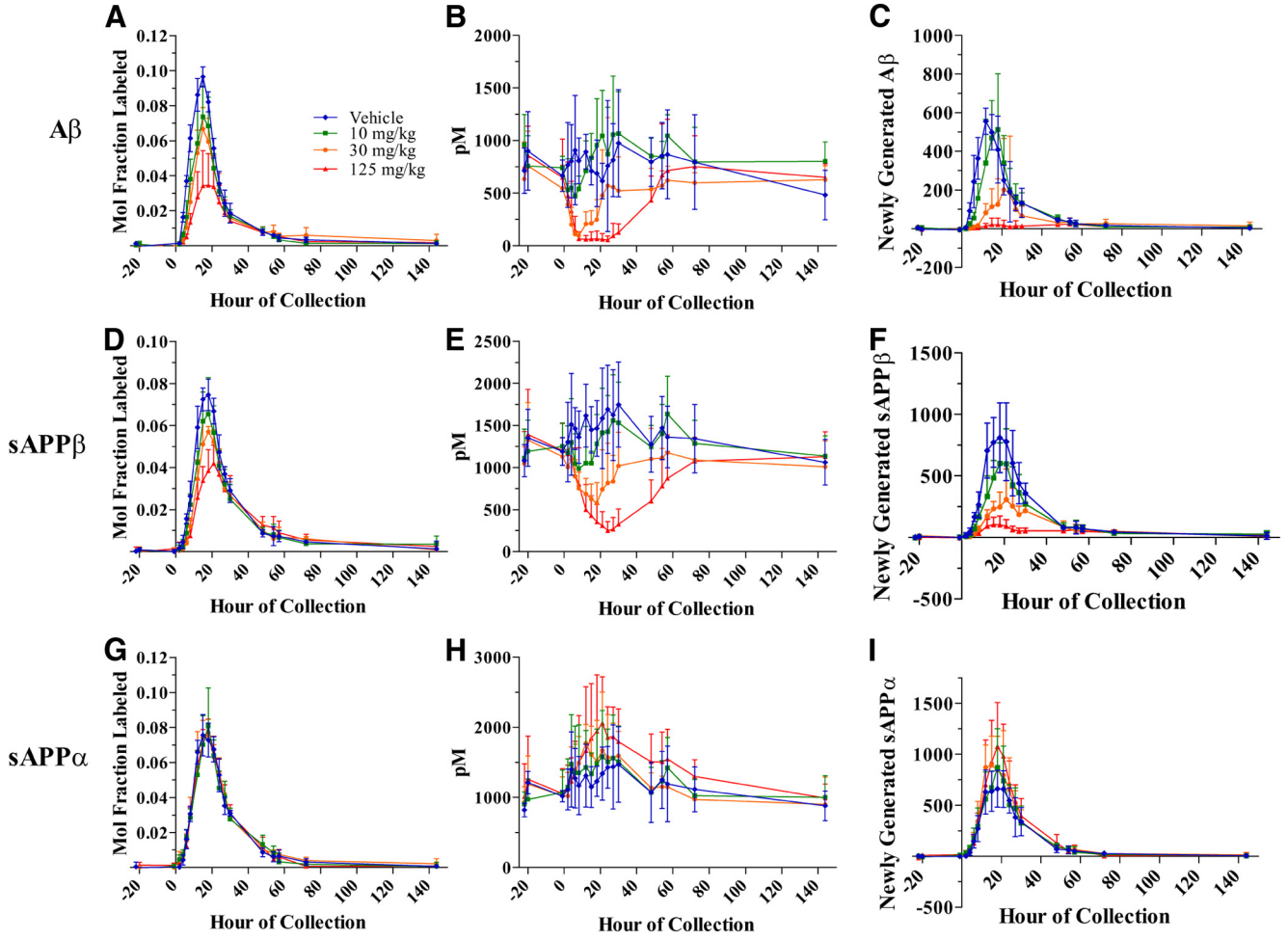

Figure 4. Effects of a BACE inhibitor on SILK relative values, ELISA absolute concentrations, and concentrations of newly generated Aβ (***A–C***), sAPPβ (***D–F***), and sAPPα (***G–I***) in CSF of NHP. ***A***, ***D***, ***G***, SILK MFL Aβ and sAPPβ decreases dose dependently with BACE inhibitor, and MFL sAPPα indicated no measurable difference among vehicle and drug groups (measured by LC-MS). ***B***, ***E***, ***H***, Concentrations of Aβ and sAPPβ decreased dose dependently and absolute concentrations of sAPPα increased dose dependently with a BACE inhibitor (measured by ELISA). ***C***, ***F***, ***I***, Newly generated Aβ and sAPPβ decreased dose dependently and newly generated sAPPα increased dose dependently with a BACE inhibitor (measured as product of LC-MS labeling and ELISA absolute concentrations at each time point). Error bars indicate SD.

Table 5. Effects of BACE inhibition on APP metabolites' AUC_{57} from SILK and ELISA assays

Dosage of BACE inhibitor	SILK MFL	ELISA concentration	Newly synthesized product (SILK % × ELISA)
Aβ (mean, SEM)			
10 mg/kg	77.8 ± 6.4%	111 ± 12.9%	88.4 ± 13.2%
30 mg/kg	70.8 ± 7.0%	58.6 ± 12.3%	37.8 ± 11.5%
125 mg/kg	47.5 ± 6.2%	33.2 ± 8.2%	9.4 ± 3.8%
sAPPβ (mean, SEM)			
10 mg/kg	84.4 ± 4.4%	88.1 ± 2.1%	71.3 ± 5.5%
30 mg/kg	78.3 ± 3.4%	63.0 ± 2.7%	42.1 ± 3.9%
125 mg/kg	69.9 ± 5.1%	38.3 ± 4.4%	17.6 ± 2.6%
sAPPα (mean, SEM)			
10 mg/kg	99.6 ± 9.3%	107.8 ± 7.4%	108.3 ± 7.6%
30 mg/kg	101.0 ± 3.2%	113.8 ± 5.8%	123.1 ± 7.4%
125 mg/kg	101.5 ± 6.6%	131.4 ± 6.9%	134.6 ± 10.1%

surrogate for human CNS APP processing. The slower turnover rates for these larger APP metabolites when compared with Aβ may be driven by delayed transport out of the brain.

In addition to the novel findings of Aβ and sAPP kinetics under steady-state conditions, this is the first report using SILK to evaluate *in vivo* APP metabolite kinetics following treatment with the BACE inhibitor MBI-5, which is distinct from Merck's BACE inhibitor MK-8931, currently in Phase 3 clinical trials. As expected, there was a notable, dose-dependent decrease in Aβ and sAPPβ in the presence of the BACE inhibitor, indicating the drug hit its intended target. The finding that there was a greater percentage reduction in Aβ compared with sAPPβ in the presence of the inhibitor was consistent with Aβ having faster kinetics at steady state (Fig. 2*D*,*E*, vehicle-treated group).

Because of conflicting results in previously reported studies that have examined both sAPPα and sAPPβ, it was unclear whether the kinetics of α-secretase processing of APP to sAPPα would also be altered in the presence of a BACE inhibitor. BACE inhibitors applied in cell culture have sometimes led to apparent shunting of APP down the α-secretase pathway resulting in increased sAPPα secretion (Hussain et al., 2007; Fukumoto et al., 2010), but not always (Kim et al., 2008). This has contrasted with human studies that seemed to indicate a noncompetitive relationship between the α-secretase and BACE APP processing pathways (Gabelle et al., 2010; Lewczuk et al., 2010; Alexopolous et al., 2012; Dobrowolska et al., 2014). Our reported baseline positive correlation of sAPPα and sAPPβ further supports this. Nevertheless, pharmacological intervention may alter normal

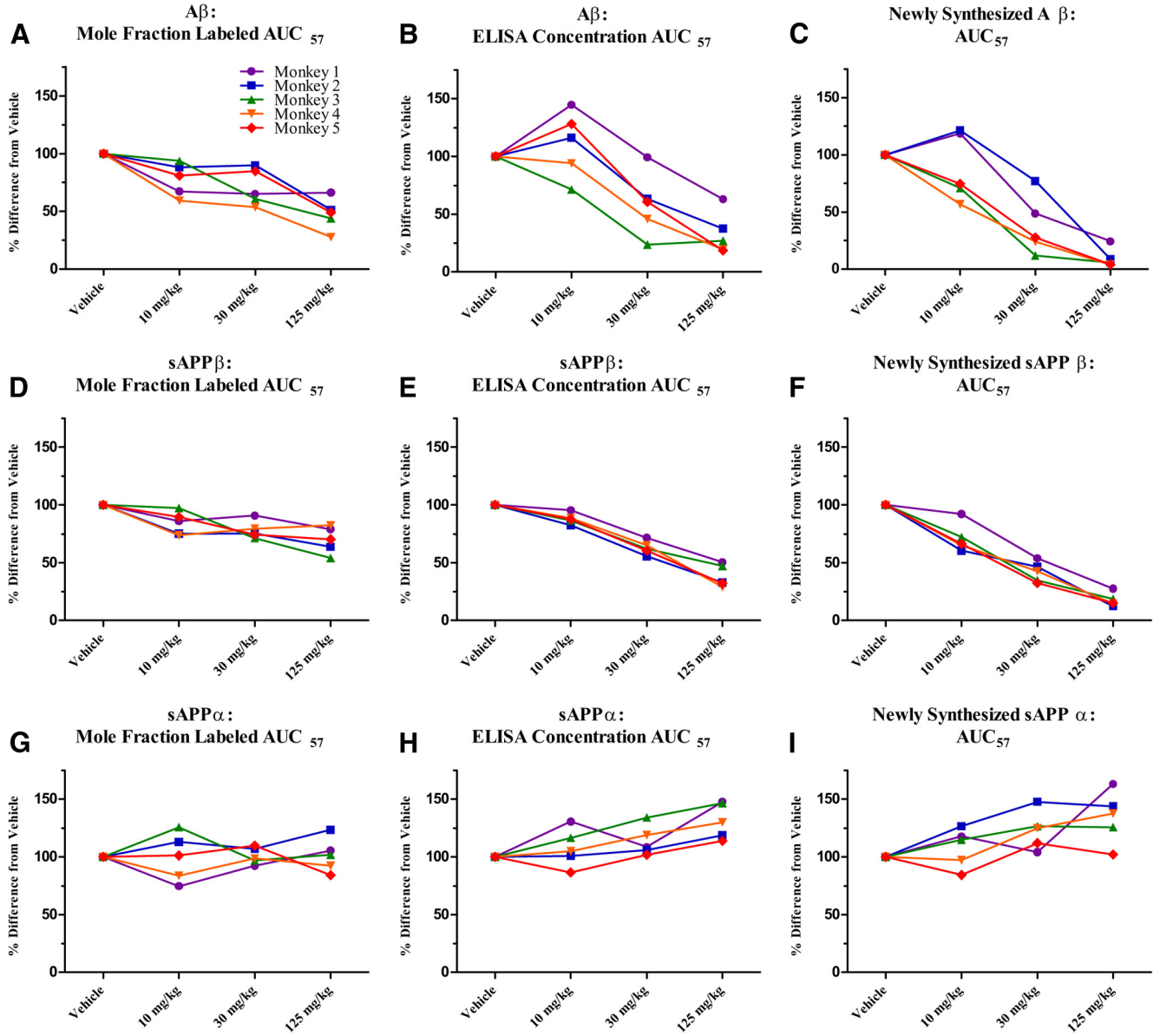

Figure 5. Effects of BACE inhibition on APP metabolites' AUC_{57}. Results are represented as percentage change from vehicle AUC_{57}. Each line represents a particular monkey. ***A***, ***D***, ***G***, MFL Aβ and sAPPβ AUC_{57} were decreased dose dependently, while MFL sAPPα AUC_{57} indicated that dosing groups did not significantly differ from the vehicle-treated group. ***B***, ***E***, ***H***, AUC_{57} values for absolute concentrations of Aβ and sAPPβ were decreased dose dependently, while AUC_{57} of absolute concentrations of sAPPα presented a dose-dependent increase. ***C***, ***F***, ***I***, AUC_{57} values for newly synthesized Aβ and sAPPβ were decreased dose dependently, while AUC_{57} of newly synthesized sAPPα presented a dose-dependent increase.

APP processing such that decreased BACE activity diverts APP into the α-secretase pathway, as demonstrated by May et al. (2011) in humans after BACE1 inhibitor LY2811376 administration resulted in an increase of CSF sAPPα corresponding to a decrease of CSF sAPPβ. Our study in NHP suggests that different APP fragment pools can manifest a spectrum of responses as supported by these findings: (1) no apparent change in the MFL sAPPα during duration of BACE inhibition used in this study (as well as a smaller degree of AUC changes in sAPPβ and Aβ) and (2) in contrast, the steady-state, absolute concentration of sAPPα demonstrated a dose-dependent sAPPα concentration increase (as well as a larger degree of AUC changes in sAPPβ and Aβ). One caveat to the ELISA measures is that sAPPα did not increase to the same extent that sAPPβ decreased (respective change from vehicle at 125 mg/kg in AUC_{57}, +35% and −83%), and there was no rebound of sAPPβ over baseline following the resumption of BACE activity as drug levels declined. Thus, a build-up of APP substrate may be degraded through mechanisms other than traditional α-secretase cleavage activities to account for these observations. For example, recent IP studies indicate that alternative α- and β-secretase processing may occur *in vivo* in human CNS, i.e., $sAPP\alpha_{Q686}$ (sAPPα′), $sAPP\alpha_{K687}$, $sAPP\beta_{M671}$, and $sAPP\beta_{Y681}$ (sAPPβ′) from the APP_{770} splice variant (Brinkmalm et al., 2013), which might not be detected with our SILK or ELISA assays. Conversely, the additional APP substrate may undergo lysosomal degradation. Measurements using SILK would not reflect APP shunted toward lysosomes, as these fragments would be unlikely to travel to CSF.

The MFL profiles of Aβ and sAPPβ were reduced in a dose-dependent manner with increasing doses of BACE inhibitor, concomitant with decreased CSF concentrations of these proteins measured by ELISA. In contrast, the MFL of sAPPα was virtually

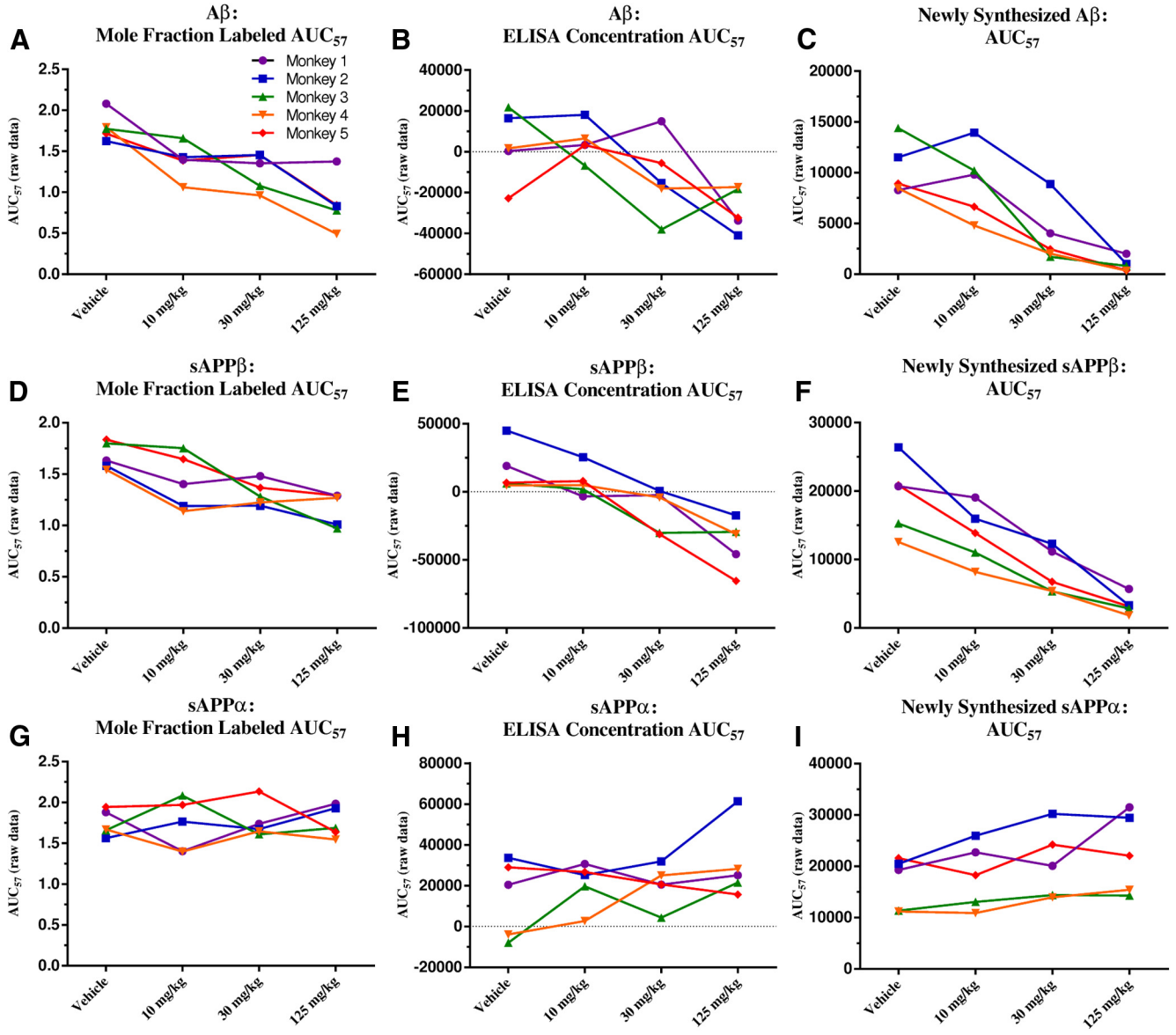

Figure 6. Effects of BACE inhibition on APP metabolites' AUC_{57} without normalization to vehicle group. Each line represents a particular monkey. ***A***, ***D***, ***G***, MFL Aβ and sAPPβ AUC_{57} were decreased dose dependently, while MFL sAPPα AUC_{57} indicated that dosing groups did not significantly differ from the vehicle-treated group. ***B***, ***E***, ***H***, AUC_{57} values for absolute concentrations of Aβ and sAPPβ were decreased dose dependently, while AUC_{57} of absolute concentrations of three monkeys' sAPPα increased. Two monkeys did not show significant changes in sAPPα. Coincidentally, these two monkeys had the lowest C_{max} for the 125 mg/kg dose among all the monkeys, and were in the lower spectrum for C_{max} at the 30 mg/kg dose. ***C***, ***F***, ***I***, AUC_{57} values for newly synthesized Aβ and sAPPβ were decreased dose dependently, while AUC_{57} of newly synthesized of sAPPα presented a dose-dependent increase.

unaltered despite a dose-dependent increase of ~30% in the ELISA concentration AUC_{57} in the highest dose group (Fig. 5*G*,*H*, Table 5). This apparent dichotomy can be explained based on simulations using nonsteady-state compartmental modeling (B.W. Patterson, J. Stone, and E.M.T. van Maanen, unpublished observations). BACE inhibitor was introduced around the same time as $^{13}C_6$-leucine tracer so the system transitioned from steady state to a nonsteady state as tracer entered the system. We may presume that the production of labeled Aβ and sAPPβ was almost immediately decreased in a dose-dependent manner as drug reached effective concentrations in the brain. The newly synthesized, $^{13}C_6$ leucine-labeled peptides moved into pools of pre-existing CSF peptides that initially remained near basal absolute concentrations, since turnover of the CSF pools must occur before CSF concentrations decrease in response to BACE inhibition. The decreased appearance of labeled Aβ and sAPPβ in CSF preceded the decrease in CSF absolute concentration, comprised of an excess of unlabeled peptides, thus resulting in a dose-dependent decrease in the labeled to unlabeled peptide ratio (i.e., isotopic enrichment). BACE inhibition should, conversely, cause the amount of APP substrate to increase, leading to increased production of sAPPα due to mass action. Thus, increasing amounts of labeled sAPPα should appear in CSF dose dependently. The absolute concentration of CSF sAPPα will increase concomitant with, and in proportion to, increased appearance of labeled sAPPα, and thus there would be little impact to the labeled to unlabeled peptide ratio. In addition to the role of CSF turnover on the differential sensitivity of both Aβ and sAPPβ enrichment profiles to acute inhibition versus an increase of sAPPα peptide synthesis, this also resulted in part because peptides were sampled from a downstream location (CSF) remote from the site of BACE activity (brain).

Further, of note is that in our study, for each metabolite, its FSR is not equal to its FCR. The FSR and FCR are imperfect indices of true turnover rate that are calculated under the assumption of a single compartmental model. However, there are many compartments in which APP may be processed and trafficked in a complex mammalian organism setting. Thus, the FSR calculations tend to be grossly underestimated and the true FSR is likely much greater than what we report and probably quite similar to our reported FCR, whose calculations are not perturbed by the added complexity of additional compartments. The FSRs and the FCRs reported here are useful in relative comparisons of the three APP metabolites in this study, but a multicompartmental model that fits the full time course could provide a closer estimate of each metabolite's true turnover rate. Such a modeling approach is currently under way.

A detailed mechanism-based, nonsteady-state PK–PD compartmental model (Danhof et al., 2005) is also in progress and will account for both the ELISA concentration data and SILK tracer enrichment time courses of APP metabolites as a function of dynamic BACE inhibition for all doses of BACE inhibitor administered, versus vehicle treatment. The model will also incorporate information from acute inhibition of γ-secretase activity (Cook et al., 2010; Van Maanen et al., 2013).

The current study has the benefit of measuring changes in APP metabolites by two separate methods: using SILK and MS, as well as measuring absolute concentrations by ELISA. SILK is a robust and reliable method of quantifying *de novo* proteins changing over time following a labeling pulse, whereas the ELISA assays measure the steady-state concentrations of a particular metabolite. SILK is more specific to newly generated proteins and more sensitive to detect changes at earlier time points in a secretase inhibitor setting (Bateman et al., 2009; Cook et al., 2010) where protein ELISA variance may mask relatively smaller changes in concentrations. Increased sensitivity of SILK is evidenced by the earlier appearance of the change in the ratio of label versus the ELISA absolute concentration changes. Additionally, SILK AUCs always had higher MTSD values than ELISA AUCs among all dose groups and metabolites.

The CNS kinetic rates of APP metabolites are an important physiologic measure that is tightly regulated and fairly consistent across primates in studies to date. Modulation of APP processing is a key approach in AD therapeutic development with BACE inhibition being an attractive target. This is consistent with recent genetic evidence of a protective factor (Jonsson et al., 2012) in individuals with a mutation at the BACE cleavage site of APP that prevents development of AD. The CNS *in vivo* study reported here indicates that BACE inhibition modulated APP processing in a predictable and dose-dependent fashion, but the study also provides a novel finding into the balance of BACE and α-secretase APP processing following BACE inhibition.

References

Alexopoulos P, Tsolakidou A, Roselli F, Arnold A, Grimmer T, Westerteicher C, Leante MR, Förstl H, Livrea P, Kurz A, Perneczky R (2012) Clinical and neurobiological correlates of soluble amyloid precursor proteins in the cerebrospinal fluid. Alzheimers Dement 8:304–311. CrossRef Medline

Bateman RJ, Munsell LY, Morris JC, Swarm R, Yarasheski KE, Holtzman DM (2006) Human amyloid-β synthesis and clearance rates as measured in cerebrospinal fluid in vivo. Nat Med 12:856–861. CrossRef Medline

Bateman RJ, Munsell LY, Chen X, Holtzman DM, Yarasheski KE (2007) Stable isotope labeling tandem mass spectrometry (SILT) to quantify protein production and clearance rates. J Am Soc Mass Spectrom 18:997–1006. CrossRef Medline

Bateman RJ, Siemers ER, Mawuenyega KG, Wen G, Browning KR, Sigurdson WC, Yarasheski KE, Friedrich SW, Demattos RB, May PC, Paul SM, Holtzman DM (2009) A gamma-secretase inhibitor decreases amyloid-β production in the central nervous system. Ann Neurol 66:48–54. CrossRef Medline

Bernier F, Sato Y, Matijevic M, Desmond H, McGrath S, Burns L, Kaplow JM, Albala B (2013) Clinical study of E2609, a novel BACE1 inhibitor, demonstrates target engagement and inhibition of BACE1 activity in CSF. Alzheimers Dement 9:P886. CrossRef

Brinkmalm G, Brinkmalm A, Bourgeois P, Persson R, Hansson O, Portelius E, Mercken M, Andreasson U, Parent S, Lipari F, Ohrfelt A, Bjerke M, Minthon L, Zetterberg H, Blennow K, Nutu M (2013) Soluble amyloid precursor protein α and β in CSF in Alzheimer's disease. Brain Res 1513:117–126. CrossRef Medline

Busciglio J, Gabuzda DH, Matsudaira P, Yankner BA (1993) Generation of beta-amyloid in the secretory pathway in neuronal and nonneuronal cells. Proc Natl Acad Sci U S A 90:2092–2096. CrossRef Medline

Cook JJ, Wildsmith KR, Gilberto DB, Holahan MA, Kinney GG, Mathers PD, Michener MS, Price EA, Shearman MS, Simon AJ, Wang JX, Wu G, Yarasheski KE, Bateman RJ (2010) Acute gamma-secretase inhibition of nonhuman primate CNS shifts Amyloid Precursor Protein (APP) metabolism from amyloid-β production to alternative APP fragments without Amyloid-β rebound. J Neurosci 30:6743–6750. CrossRef Medline

Cumming JN, Smith EM, Wang L, Misiaszek J, Durkin J, Pan J, Iserloh U, Wu Y, Zhu Z, Strickland C, Voigt J, Chen X, Kennedy ME, Kuvelkar R, Hyde LA, Cox K, Favreau L, Czarniecki MF, Greenlee WJ, McKittrick BA, et al. (2012) Structure based design of iminohydantoin BACE1 inhibitors: identification of an orally available, centrally active BACE1 inhibitor. Bioorg Med Chem Lett 22:2444–2449. CrossRef Medline

Danhof M, Alvan G, Dahl SG, Kuhlmann J, Paintaud G (2005) Mechanism-based pharmacokinetic-pharmacodynamic modeling-a new classification of biomarkers. Pharm Res 22:1432–1437. CrossRef Medline

Dobrowolska J, Mawuenyega KG, Bateman RJ (2008) The metabolism of amyloid precursor protein as measured in human cerebrospinal fluid. Soc Neurosci Abstr 34:138.2.

Dobrowolska JA, Kasten T, Huang Y, Benzinger TL, Sigurdson W, Ovod V, Morris JC, Bateman RJ (2014) Diurnal patterns of soluble amyloid precursor protein metabolites in the human central nervous system. PLoS One 9:e89998. CrossRef Medline

Egan MF, Forman MS, Palcza J, Tseng J, Leempoels J, Ramael S, Han D, Jhee S, Ereshefsky L, Tanen M, Laterza O, Dockendorf M, Krishna G, Ma L, Wagner JA, Troyer MD (2012) The novel BACE inhibitor MK-8931 dramatically lowers CSF Aβ peptides in healthy subjects following single and multiple dose administration. 5th conference clinical trials on Alzheimer's disease: October 29–31, 2012, Grimaldi Forum, Convention Center, Monte Carlo. J Nutr Health Aging 16:797. CrossRef

Forman MS, Palcza J, Tseng J, Dockendorf M, Canales C, Apter J, Backonja M, Bryan E, Ereshefsky L, Gevorkyan H, Jhee S, Ostler R, Zari A, Kleijn HJ, Laterza O, Ma L, Stone J, Tanen M, Wagner JA, Troyer MD (2013) The novel BACE inhibitor MK-8931 dramatically lowers CSF Aβ peptide in patients with mild to moderate Alzheimer's disease. AD/PD™ 2013, the 11th International Conference on Alzheimer's and Parkinson's Diseases, Florence, Italy.

Fukumoto H, Cheung BS, Hyman BT, Irizarry MC (2002) β-secretase protein and activity are increased in the neocortex in Alzheimer disease. Arch Neurol 59:1381–1389. CrossRef Medline

Fukumoto H, Takahashi H, Tarui N, Matsui J, Tomita T, Hirode M, Sagayama M, Maeda R, Kawamoto M, Hirai K, Terauchi J, Sakura Y, Kakihana M, Kato K, Iwatsubo T, Miyamoto M (2010) A noncompetitive BACE1 inhibitor TAK-070 ameliorates Abeta pathology and behavioral deficits in a mouse model of Alzheimer's disease. J Neurosci 30:11157–11166. CrossRef Medline

Gabelle A, Roche S, Gény C, Bennys K, Labauge P, Tholance Y, Quadrio I, Tiers L, Gor B, Chaulet C, Vighetto A, Croisile B, Krolak-Salmon P, Touchon J, Perret-Liaudet A, Lehmann S (2010) Correlations between soluble α/β forms of amyloid precursor protein and Aβ38, 40, and 42 in human cerebrospinal fluid. Brain Res 1357:175–183. CrossRef Medline

Gilberto DB, Zeoli AH, Szczerba PJ, Gehret JR, Holahan MA, Sitko GR, Johnson CA, Cook JJ, Motzel SL (2003) An alternative method of chronic cerebrospinal fluid collection via the cisterna magna in conscious rhesus monkeys. Contemp Top Lab Anim Sci 42:53–59. Medline

Holsinger RM, Lee JS, Boyd A, Masters CL, Collins SJ (2006) CSF BACE1 activity is increased in CJD and Alzheimer disease versus other dementias. Neurology 67:710–712. CrossRef Medline

Hussain I, Hawkins J, Harrison D, Hille C, Wayne G, Cutler L, Buck T, Walter D, Demont E, Howes C, Naylor A, Jeffrey P, Gonzalez MI, Dingwall C, Michel A, Redshaw S, Davis JB (2007) Oral administration of a potent and selective non-peptidic BACE-1 inhibitor decreases beta-cleavage of amyloid precursor protein and amyloid-beta production *in vivo*. J Neurochem 100:802–809. CrossRef Medline

Irizarry MC, Locascio JJ, Hyman BT (2001) β-site APP cleaving enzyme mRNA expression in APP transgenic mice: anatomical overlap with transgene expression and static levels with aging. Am J Pathol 158:173–177. CrossRef Medline

Jonsson T, Atwal JK, Steinberg S, Snaedal J, Jonsson PV, Bjornsson S, Stefansson H, Sulem P, Gudbjartsson D, Maloney J, Hoyte K, Gustafson A, Liu Y, Lu Y, Bhangale T, Graham RR, Huttenlocher J, Bjornsdottir G, Andreassen OA, Jönsson EG, et al. (2012) A mutation in APP protects against Alzheimer's disease and age-related cognitive decline. Nature 488:96–99. CrossRef Medline

Kim ML, Zhang B, Mills IP, Milla ME, Brunden KR, Lee VM (2008) Effects of TNFα-converting enzyme inhibition on amyloid β production and APP processing *in vitro* and *in vivo*. J Neurosci 28:12052–12061. CrossRef Medline

Lewczuk P, Kamrowski-Kruck H, Peters O, Heuser I, Jessen F, Popp J, Bürger K, Hampel H, Frölich L, Wolf S, Prinz B, Jahn H, Luckhaus Ch, Perneczky R, Hüll M, Schröder J, Kessler H, Pantel J, Gertz HJ, Klafki HW, et al. (2010) Soluble amyloid precursor proteins in the cerebrospinal fluid as novel potential biomarkers of Alzheimer's disease: a multicenter study. Mol Psychiatry 15:138–145. CrossRef Medline

Li R, Lindholm K, Yang LB, Yue X, Citron M, Yan R, Beach T, Sue L, Sabbagh M, Cai H, Wong P, Price D, Shen Y (2004) Amyloid β peptide load is correlated with increased β-secretase activity in sporadic Alzheimer's disease patients. Proc Natl Acad Sci U S A 101:3632–3637. CrossRef Medline

Malamas MS, Robichaud A, Erdei J, Quagliato D, Solvibile W, Zhou P, Morris K, Turner J, Wagner E, Fan K, Olland A, Jacobsen S, Reinhart P, Riddell D, Pangalos M (2010) Design and synthesis of aminohydantoins as potent and selective human β-secretase (BACE1) inhibitors with enhanced brain permeability. Bioorg Med Chem Lett 20:6597–6605. CrossRef Medline

Mandal M, Zhu Z, Cumming JN, Liu X, Strickland C, Mazzola RD, Caldwell JP, Leach P, Grzelak M, Hyde L, Zhang Q, Terracina G, Zhang L, Chen X, Kuvelkar R, Kennedy ME, Favreau L, Cox K, Orth P, Buevich A, et al. (2012) Design and validation of bicyclic iminopyrimidinones as beta amyloid cleaving enzyme-1 (BACE1) inhibitors: conformational constraint to favor a bioactive conformation. J Med Chem 55:9331–9345. CrossRef Medline

Mattsson N, Rajendran L, Zetterberg H, Gustavsson M, Andreasson U, Olsson M, Brinkmalm G, Lundkvist J, Jacobson LH, Perrot L, Neumann U, Borghys H, Mercken M, Dhuyvetter D, Jeppsson F, Blennow K, Portelius E (2012) BACE1 inhibition induces a specific cerebrospinal fluid β-amyloid pattern that identifies drug effects in the central nervous system. PLoS One 7:e31084. CrossRef Medline

May PC, Dean RA, Lowe SL, Martenyi F, Sheehan SM, Boggs LN, Monk SA, Mathes BM, Mergott DJ, Watson BM, Stout SL, Timm DE, Smith Labell E, Gonzales CR, Nakano M, Jhee SS, Yen M, Ereshefsky L, Lindstrom TD, Calligaro DO, et al. (2011) Robust central reduction of Amyloid-β in humans with an orally available, non-peptidic β-secretase inhibitor. J Neurosci 31:16507–16516. CrossRef Medline

Mawuenyega KG, Sigurdson W, Ovod V, Munsell L, Kasten T, Morris JC, Yarasheski KE, Bateman RJ (2010) Decreased clearance of CNS beta-amyloid in Alzheimer's disease. Science 330:1774. CrossRef Medline

Oltersdorf T, Ward PJ, Henriksson T, Beattie EC, Neve R, Lieberburg I, Fritz LC (1990) The Alzheimer amyloid precursor protein. Identification of a stable intermediate in the biosynthetic/degradative pathway. J Biol Chem 265:4492–4497. Medline

Ortega F, Stott J, Visser SA, Bendtsen C (2013) Interplay between α-, β-, and γ-secretases determines biphasic amyloid-β protein level in the presence of a γ-secretase inhibitor. J Biol Chem 288:785–792. CrossRef Medline

Perez RG, Squazzo SL, Koo EH (1996) Enhanced release of amyloid β-protein from codon 670/671 "Swedish" mutant β-amyloid precursor protein occurs in both secretory and endocytic pathways. J Biol Chem 271:9100–9107. CrossRef Medline

Portelius E, Price E, Brinkmalm G, Stiteler M, Olsson M, Persson R, Westman-Brinkmalm A, Zetterberg H, Simon AJ, Blennow K (2011) A novel pathway for amyloid precursor protein processing. Neurobiol Aging 32:1090–1098. CrossRef Medline

Potter R, Patterson BW, Elbert DL, Ovod V, Kasten T, Sigurdson W, Mawuenyega K, Blazey T, Goate A, Chott R, Yarasheski KE, Holtzman DM, Morris JC, Benzinger TL, Bateman RJ (2013) Increased in vivo amyloid-β42 production, exchange, and loss in presenilin mutation carriers. Sci Transl Med 5:189ra77. CrossRef Medline

Rosén C, Andreasson U, Mattsson N, Marcusson J, Minthon L, Andreasen N, Blennow K, Zetterberg H (2012) Cerebrospinal fluid profiles of amyloid β-related biomarkers in Alzheimer's disease. Neuromolecular Med 14:65–73. CrossRef Medline

Sankaranarayanan S, Holahan MA, Colussi D, Crouthamel MC, Devanarayan V, Ellis J, Espeseth A, Gates AT, Graham SL, Gregro AR, Hazuda D, Hochman JH, Holloway K, Jin L, Kahana J, Lai MT, Lineberger J, McGaughey G, Moore KP, Nantermet P, et al. (2009) First demonstration of cerebrospinal fluid and plasma Aβ lowering with oral administration of a β-site amyloid precursor protein-cleaving enzyme 1 inhibitor in nonhuman primates. J Pharmacol Exp Ther 328:131–140. CrossRef Medline

Savage M, Holder D, Wu G, Kaplow JM, Siuciak J, Potter W, Alzheimer's Disease Neuroimaging Initiative (ADNI), Foundation for NIH Biomarkers Consortium CSF Proteomics Project Team (2013) Soluble BACE activity and sAPPβ levels do not differentiate Alzheimer's disease and age-matched control cerebrospinal fluid in the ADNI-1 cohort. Alzheimers Dement 9:P201. CrossRef

Stamford AW, Scott JD, Li SW, Babu S, Tadesse D, Hunter R, Wu Y, Misiaszek J, Cumming JN, Gilbert EJ, Huang C, McKittrick BA, Hong L, Guo T, Zhu Z, Strickland C, Orth P, Voigt JH, Kennedy ME, Chen X, et al. (2012) Discovery of an orally available, brain penetrant BACE1 inhibitor that affords robust CNS Aβ reduction. ACS Med Chem Lett 3:897–902. CrossRef Medline

Takahashi H, Fukumoto H, Maeda R, Terauchi J, Kato K, Miyamoto M (2010) Ameliorative effects of a non-competitive BACE1 inhibitor TAK-070 on Aβ peptide levels and impaired learning behavior in aged rats. Brain Res 1361:146–156. CrossRef Medline

Truong AP, Tóth G, Probst GD, Sealy JM, Bowers S, Wone DW, Dressen D, Hom RK, Konradi AW, Sham HL, Wu J, Peterson BT, Ruslim L, Bova MP, Kholodenko D, Motter RN, Bard F, Santiago P, Ni H, Chian D, et al. (2010) Design of an orally efficacious hydroxyethylamine (HEA) BACE-1 inhibitor in a preclinical animal model. Bioorg Med Chem Lett 20:6231–6236. CrossRef Medline

Van Maanen E, van Steeg T, Ahsman M, Savage MJ, Michener MS, Kleijn HJ, Danhof M, Stone J (2013) A systems pharmacology model of the APP processing pathway in Alzheimer's Disease. American Conference on Pharmacometrics, Ft. Lauderdale, FL.

Verheijen JH, Huisman LG, van Lent N, Neumann U, Paganetti P, Hack CE, Bouwman F, Lindeman J, Bollen EL, Hanemaaijer R (2006) Detection of a soluble form of BACE-1 in human cerebrospinal fluid by a sensitive activity assay. Clin Chem 52:1168–1174. CrossRef Medline

Weidemann A, König G, Bunke D, Fischer P, Salbaum JM, Masters CL, Beyreuther K (1989) Identification, biogenesis, and localization of precursors of Alzheimer's disease A4 amyloid protein. Cell 57:115–126. CrossRef Medline

Wolfe RR, Chinkes DL (2005) Isotope tracers in metabolic research: principles and practice of kinetic analysis, Ed 2. Hoboken, NJ: Wiley.

Wu G, Sankaranarayanan S, Hsieh SH, Simon AJ, Savage MJ (2011) Decrease in brain soluble amyloid precursor protein β (sAPPβ) in Alzheimer's disease cortex. J Neurosci Res 89:822–832. CrossRef Medline

Wu G, Sankaranarayanan S, Wong J, Tugusheva K, Michener MS, Shi X, Cook JJ, Simon AJ, Savage MJ (2012) Characterization of plasma β-secretase (BACE1) activity and soluble amyloid precursor proteins as potential biomarkers for Alzheimer's disease. J Neurosci Res 90:2247–2258. CrossRef Medline

Yang LB, Lindholm K, Yan R, Citron M, Xia W, Yang XL, Beach T, Sue L, Wong P, Price D, Li R, Shen Y (2003) Elevated β-secretase expression and enzymatic activity detected in sporadic Alzheimer disease. Nat Med 9:3–4. CrossRef Medline

Yarasheski KE, Smith K, Rennie MJ, Bier DM (1992) Measurement of muscle protein fractional synthetic rate by capillary gas chromatography/combustion isotope ratio mass spectrometry. Biol Mass Spectrom 21:486–490. CrossRef Medline

Zetterberg H, Andreasson U, Hansson O, Wu G, Sankaranarayanan S, Andersson ME, Buchhave P, Londos E, Umek RM, Minthon L, Simon AJ, Blennow K (2008) Elevated cerebrospinal fluid BACE1 activity in incipient Alzheimer disease. Arch Neurol 65:1102–1107. CrossRef Medline